

Prediction of hydraulic and petrophysical parameters from indirect measurements of electrical resistivity to determine soil-water retention curve – studies in granular soils

Manuelle Santos Góis¹ , Katherin Rocio Cano Bezerra da Costa¹ ,
André Luís Brasil Cavalcante^{1#} 

Article

Keywords

Indirect measures
Hydrogeophysical functions
Electrical resistivity
characteristic curve
Petrophysical relationships
Granular soil

Abstract

The characterization of unsaturated soils using hydromechanical methods is an essential requirement in soil science. However, current laboratory techniques used to obtain soil water retention and unsaturated hydraulic conductivity curves are time-consuming. To address this issue, a method based on indirect measures (electrical resistivity/electrical conductivity) was developed to quantitatively characterize soils. A novel unsaturated semi-empirical hydrogeophysical model of soils was developed by incorporating the hydrodynamic, geophysical, and petrophysical characteristics of soils. The model assumes that the parameters influencing the variation in the volumetric water content with matric suction and electrical resistivity are the same. The electrical resistivity characteristic curve (ERCC) defines a function that correlates environmental variables, electrical resistivity, soil water status, matric suction, hydraulic and petrophysical parameters, and fluid electrical resistivity. Model validation confirmed that the proposed approach can estimate the soil water retention curve (SWRC) via the indirect measures, and the results agreed with the experimental data. This indicates that it is possible to determine the SWRC and unsaturated hydraulic conductivity function of soil using the described approach.

1. Introduction

The characterization and comprehension of Earth's surface dynamics are fundamental in various fields, such as civil engineering. Human activities that modify the soil surface can induce changes in the hydraulic and mechanical properties of materials, reducing the soil's natural infiltration capacity. Such changes influence natural processes, including surface flow, evapotranspiration, groundwater recharge, soil erosion, and contaminants' transport in both surface and groundwater (Fredlund & Rahardjo, 1993; Libardi, 2005; Briaud, 2013; Camapum de Carvalho & Gitirana Junior, 2021; Fredlund, 2021; Carbajal et al., 2022). To tackle this issue, several fields, including geotechnical engineering, geology, geophysics, and hydrology, have utilized numerical and conceptual models to approximate the physical phenomenon of near-surface flux (Liu, 2017). Nonetheless, accurately defining the soil water retention curves and unsaturated hydraulic conductivity function poses a critical challenge in hydrogeological modeling.

Numerous publications have employed indirect measures on porous media to comprehend and depict the soil's saturated and unsaturated states. Mualem & Friedman (1991), Lesmes & Friedman (2005), Hinnell et al. (2010), Revil et al. (2012), and Binley et al. (2015) conducted hydrogeophysical investigations to examine the correlation between electrical parameters and hydrogeological properties of saturated and unsaturated media for the prediction of hydraulic parameters.

Shah & Singh (2005) and Hong-jing et al. (2014) established correlations between electrical conductivity/resistivity and degree of saturation/soil volumetric water content. Di Maio et al. (2015) proposed a combined utilization of Archie's law (Archie, 1942) and van Genuchten's model (van Genuchten, 1980) to relate electrical resistivity to hydraulic conductivity. Fu et al. (2021b) developed a generalized form of Archie's law that describes the correlation between soil electrical conductivity and volumetric water content. Doussan & Ruy (2009), Piegari & Di Maio (2013), Mawer et al. (2015), Niu et al. (2015), and Cardoso & Dias (2017) conducted studies for the prediction of unsaturated hydraulic conductivity and matric potential from electrical

[#]Corresponding author. E-mail address: abrasil@unb.br

¹Universidade de Brasília, Departamento de Engenharia Civil e Ambiental, Brasília, DF, Brasil.

Submitted on December 4, 2022; Final Acceptance on May 26, 2023; Discussion open until November 30, 2023.

<https://doi.org/10.28927/SR.2023.013822>



This is an Open Access article distributed under the terms of the Creative Commons Attribution License, which permits unrestricted use, distribution, and reproduction in any medium, provided the original work is properly cited.

conductivity data. Kong et al. (2017), Lu et al. (2020), and Fu et al. (2021a) established functions for the electrical resistivity/electrical conductivity that depend on the volumetric water content and obtained the soil's characteristic curve.

This study presents a novel unsaturated semi-empirical hydrogeophysical model of soils that is based on the hypothesis that the parameters that impact the alteration in the volumetric water content with matric suction and electrical resistivity are the same. These hydrogeophysical functions demonstrate that it is feasible to depict a medium's state through indirect measurements and acquire soil water retention and hydraulic conductivity curves in an unsaturated state.

The validation conducted demonstrates that the proposed hydrogeophysical model can indirectly estimate the water retention curve and unsaturated hydraulic conductivity function of soil using electrical resistivity measurements with low computational and operational cost and in a timely manner.

2. Soils in the unsaturated zone

The vadose zone refers to the region between the ground surface and the water table. In simple terms, subsurface water is distributed in the soil voids, forming the unsaturated zone. Within this region, the surface part of the geological material, which lies between the land's surface and the top of the aquifer, has pores filled with both liquid and gaseous water. However, the capillary fringe immediately above the water table is predominantly saturated. In these soils, the impact of pore pressure is negative and determined by the cumulative effects of thermal, gravitational, kinetic, pressure, pneumatic, matric, and osmotic potentials. Among these factors, osmotic and matric suction play critical roles in determining the hydromechanical properties of unsaturated soils.

The suction effect is physically equivalent to an external pressure that influences the stress state of a material, resulting in an increase in soil strength as suction rises (Fredlund & Rahardjo, 1993; Cavalcante & Mascarenhas, 2021). Matric suction, which depends on capillarity's physical phenomenon, is determined by the degree of soil saturation and the void structure within the soil, which is the main factor responsible for negative pore pressure. Hence, the water state in the soil, as determined by infiltration and percolation, substantially contributes to matric suction. Understanding and enhancing current techniques for determining the volumetric water content-to-suction ratio are crucial, as the relationship between suction and soil processes highlights its significance. The volumetric water content is currently defined using a soil water retention curve (SWRC), and the hydraulic conductivity-suction ratio is established based on the unsaturated hydraulic conductivity function (Fredlund & Rahardjo, 1993; Sheng et al., 2008; Cho, 2016; Crawford et al., 2019; Chou & Wang, 2021; Albuquerque et al., 2022).

2.1 Unsaturated flow constitutive model

Richards equation (Richards, 1931) is commonly utilized in soil science for modeling unsaturated flow. However, the nonlinearity of the constitutive relationships between hydraulic conductivity-suction and volumetric water content-suction hinders analytical solutions to the problem. To address this issue, researchers, such as Brooks & Corey (1964), van Genuchten (1980), and Fredlund & Xing (1994), have attempted to consolidate some of the constitutive models to enable numerical solutions to the partial differential equation for unsaturated flow. Meanwhile, other studies have presented analytical solutions limited to specific cases, such as stationary flow under simplified hydraulic conditions, which leads to a loss of the porous medium's transient approach to the flow problem (Lai & Ogden, 2015; Zhang et al., 2016).

To accurately model transient unsaturated flow, Cavalcante et al. (2019) presented one-, two-, and three-dimensional analytical solutions based on the theory developed by Cavalcante & Zornberg (2017). These authors developed a series of analytical solutions to the problem of transient one-dimensional unsaturated flow, making the following assumptions: (i) volumetric changes of unsaturated soils in the presence of flow are ignored; (ii) soil porosity remains constant in any wetting or drying cycle; (iii) the volumetric water content is an independent variable. Consequently, it is possible to transform the Richards equation into a one-dimensional flow in the z-direction:

$$\frac{\partial \theta}{\partial t} = \frac{\partial}{\partial z} \left(\frac{k_z(\theta)}{g \rho_w} \frac{\partial \psi}{\partial \theta} \frac{\partial \theta}{\partial z} \right) - \frac{\partial k_z(\theta)}{\partial z} \quad (1)$$

where θ = the volumetric soil water content (L^3L^{-3}), t = the time (T); ψ = the soil suction ($ML^{-1}T^{-2}$); g = the acceleration due to gravity (LT^{-2}); ρ_w = the water density (ML^{-3}); $k_z(\theta)$ = the unsaturated hydraulic conductivity function in terms of the volumetric water content in the z-direction (LT^{-1}), and $\partial \psi / \partial \theta$ = the variation in the matric suction concerning the volumetric water content.

Cavalcante & Zornberg (2017) established the constitutive models that physically represent the soil water retention curve and unsaturated hydraulic conductivity function to derive the analytical solutions for the one-dimensional unsaturated flow equation. These models consider a uniform pore distribution that corresponds to the soil macro-porosity of tropical regions. The models provide a clear and concise definition of the physical behaviors of the correlated properties:

$$\theta(\psi) = \theta_r + (\theta_s - \theta_r) \cdot \exp(-|\psi| \cdot \delta) \quad (2)$$

where θ_s = the volumetric soil water content in the saturated state (L^3L^{-3}); θ_r = the volumetric soil water content in the

residual state (L^3L^{-3}); $(\theta_s - \theta_r)$ = the maximum soil wetting capacity (L^3L^{-3}); and δ = the hydraulic adjustment parameter ($M^{-1}LT^2$). The unsaturated hydraulic conductivity function describes the rate at which fluid seeps through an unsaturated porous medium, as given by:

$$k(\psi) = k_{sat} \cdot \exp(-|\psi| \cdot \delta) \quad (3)$$

where k_{sat} = the saturated hydraulic conductivity of the soil (LT^{-1}). In unsaturated soils, the unsaturated hydraulic conductivity is contingent upon the pore structure and size, the volume of water present in the medium, and the saturation history. Hence, soils with larger voids (i.e., granular material) are more prone to moisture reduction under pressure application, resulting in significant reductions in hydraulic conductivity, which directly influences the hydromechanical behavior.

The hydraulic adjustment parameter δ refers to the initial angular coefficient of the curves determined by the constitutive model. It is directly affected by the maximum soil wetting capacity and the saturated hydraulic conductivity. Costa & Cavalcante (2020) established an analytical correlation between the air-entry and the δ parameter, expressed as:

$$\psi_{air} = \frac{\exp(1 - \exp(1))}{\delta} \quad (4)$$

where ψ_{air} = the air-entry soil suction ($ML^{-1}T^{-2}$).

Hence, by knowing the δ parameter, it is feasible to ascertain the air-entry soil suction value and thereby estimate the magnitude of the capillary zone in the porous medium.

2.2 Electrical properties of near-surface soils

Geophysical properties or attributes have emerged as potent tools for characterizing the environment in diverse research domains, such as geology, archaeology, oceanography, engineering, and agronomy. For instance, electrical attributes are utilized to identify hydrocarbon-producing wells, underground water, contamination, and building foundations. Based on petrophysical relationships, these attributes enable rapid and indirect characterization of the environment from physical, mechanical, and hydraulic standpoints (Telford et al., 1990; Hubbard & Rubin, 2005; Glover, 2015).

Soil electrical attributes can be measured using electronic, dielectric, or electrolytic techniques. Electromagnetically, soil can be viewed as heterogeneous composites of conductive and/or dielectric solid particles surrounded by aqueous electrolytes in varying proportions. Thus, the electrical properties of soil depend on the mineral composition and texture of the solid matrix, which encompasses properties such as structure, void ratio, salt and fluid concentration, temperature, and pore-space geometry, along with the

volumetric water content in the voids (Keller & Frischknecht, 1966; Rhoades et al., 1976; Keller, 1988; Telford et al., 1990; Butler, 2005; Friedman, 2005; Lima, 2014). These properties also influence the mechanical and hydraulic traits of soils.

Archie (1942) developed empirical laws that establish connections between the electrical resistivity of rock, its porosity, the resistivity of the water that saturates its pores, and the degree of saturation of the pore space.

The two laws formulated by Archie can be merged into a single equation (Glover, 2015), as given by:

$$ER = ER_w n^{-m} S_w^{-p} \quad (5)$$

where ER = the electrical resistivity of an unsaturated sample ($ML^3T^{-1}Q^{-2}$); ER_w = the fluid electrical resistivity ($ML^3T^{-1}Q^{-2}$), n = the porosity, which is the ratio of the volume of voids to the total volume (non-dimensional), m = the cementation exponent (non-dimensional), p = the saturation exponent (non-dimensional), S_w = the degree of saturation (non-dimensional).

Several empirical equations and physical models have been suggested in the literature to estimate the electrical resistivity of soil mixtures as a function of the degree of saturation or volumetric water content. For low-specific-surface soils (with negligible surface conductivity), such as clean sands, Archie's law is widely employed. However, it is essential to note that Archie's law is applicable only when the liquid phase is continuous, in the funicular state, and it is inadequate when the lithology consists of minerals, usually shales, that provide a substantial surface conductance.

Various studies have employed these empirical relationships to establish a law for unsaturated porous environments, relating the volumetric water content, fluid electrical conductivity, petrophysical parameters, and the electrical conductivity of an unsaturated medium (Glover et al., 2000; Santamarina et al., 2001; Rinaldi & Cuestas, 2002; Shah & Singh, 2005; Ewing & Hunt, 2006; Glover, 2010; Kibria & Hossain, 2012; Glover, 2015; Singha et al., 2014; Datsios et al., 2017). Glover (2015) has proposed the following relationship:

$$ER = \tau \cdot n^{-m} \cdot ER_w \cdot S_w^{-p} \quad (6)$$

where τ = the tortuosity, which is related to the path length of the current flow (non-dimensional).

Equation 6 can be alternatively written in terms of electrical conductivity (inverse of electrical resistivity), as follows:

$$EC = EC_w \cdot (\tau \cdot n^{-m} \cdot S_w^{-p})^{-1} \quad (7)$$

where EC_w = the fluid electrical conductivity ($M^{-1}L^{-3}T Q^2$).

Hence, Equation 6 can be rephrased and expressed in terms of the soil's volumetric water content, as follows:

$$\theta(ER) = \left(\frac{ER}{\tau \cdot n^{-m+p} \cdot ER_w} \right)^{-1/p} \quad (8)$$

In granular soils, which are the subject of this study, the electrical conductivity or resistivity of a soil sample is mainly influenced by the fluid's nature, the proportion of voids in the sample, the particle distribution, the salt concentration in the fluid, and the degree of saturation. Hence, it is feasible to illustrate how the electrical resistivity varies as a function of the volumetric water content of the soil. This study aims to establish a hydrogeophysical model based on indirect electrical measurements to characterize a soil's hydraulic and petrophysical environment.

3. Unsaturated semi-empirical hydrogeophysical model of soils

The hydrogeophysical model of soils proposed in this study builds upon the hydrogeomechanical model developed by Cavalcante & Zornberg (2017) and the empirical relationship between the volumetric water content and electrical resistivity. The model operates under the assumption that the parameters influencing the variations in the volumetric water content with both matric suction and electrical resistivity are equivalent. By combining Equations 2 and 8, the model establishes a function that correlates several environmental variables, such as electrical resistivity, soil water content, matric suction, hydraulic and petrophysical parameters, and the electrical resistivity of the fluid within a porous medium. It can be written as:

$$ER(\psi) = \frac{\tau \cdot n^{-m+p} \cdot ER_w}{\left(\theta_r + (\theta_s - \theta_r) \cdot \exp(-|\psi| \cdot \delta) \right)^p} \quad (9)$$

Equation 9 represents a semi-analytical constitutive model for the Electrical Resistivity Characteristic Curve (ERCC) as a function of the soil's electrical and hydraulic characteristics, as well as petrophysical parameters (τ , n , m , and p). When setting ψ to zero, the starting point of the ERCC is obtained, which includes contributions from θ_s , ER_w , and petrophysical parameters, i.e., $ER(0) = \tau \cdot n^{-m+p} \cdot \theta_s^{-p} \cdot ER_w$. In Equation 9, the slope, $\partial ER(\psi) / \partial \psi$, approaches zero as $ER(\psi)$ approaches its residual and saturated states.

The characteristic curves for hydraulic and hydrogeophysical parameters (Figure 1) exhibit a correspondence between the residual and saturated states and the air-entry point. At low levels of matric suction, indicating a higher water content in the system, the electrical resistivity values are lower (Figure 1). As the matric suction increases, corresponding to the air-entry point of 0.28 kPa (determined using Equation 4 for $\delta = 0.65 \text{ kPa}^{-1}$), the electrical resistivity begins to increase

while the water content in the system decreases to the interstitial volumetric water content state (Figure 1).

The hydrogeophysical function for unsaturated hydraulic conductivity as a function of the electrical resistivity was determined using Equations 2, 3, and 8, and is expressed as follows:

$$k_{us}(ER) = \begin{cases} k_{sat}, & \text{if } ER < ER_w \cdot \theta_s^{-p} \cdot \tau \cdot n^{-m+p} \\ \frac{k_{sat}}{\theta_s - \theta_r} \left(\left(\frac{ER}{\tau \cdot n^{-m+p} \cdot ER_w} \right)^{-1/p} - \theta_r \right), & \text{if } ER \geq ER_w \cdot \theta_s^{-p} \cdot \tau \cdot n^{-m+p} \end{cases} \quad (10)$$

Equation 10 describes the unsaturated hydraulic conductivity as a function of electrical resistivity and dependent on hydraulic and petrophysical parameters. If the electrical resistivity (ER) is less than $ER_w \cdot \theta_s^{-p} \cdot \tau \cdot n^{-m+p}$, then $k_{us}(ER) = k_{sat}$, indicating a high volumetric water content and thus low soil resistivity. However, if ER is greater than or equal to $ER_w \cdot \theta_s^{-p} \cdot \tau \cdot n^{-m+p}$, the unsaturated hydraulic conductivity decreases with increasing electrical resistivity.

At higher levels of electrical resistivity ($ER > 220.38 \text{ } \Omega \cdot \text{m}$), there is a noticeable reduction in unsaturated hydraulic conductivity, and it remains constant after reaching $1000 \text{ } \Omega \cdot \text{m}$ (Figure 2).

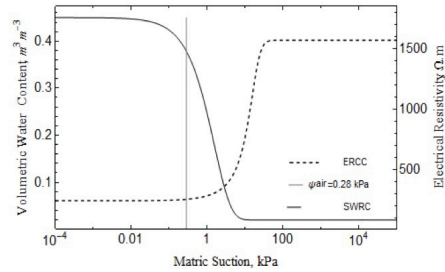


Figure 1. SWRC and ERCC characteristic curves for a sandy soil with parameters: $\theta_r = 0.02 \text{ m}^3 \cdot \text{m}^{-3}$, $\theta_s = 0.45 \text{ m}^3 \cdot \text{m}^{-3}$, $\delta = 0.65 \text{ kPa}^{-1}$ ($\psi_{air} = 0.28 \text{ kPa}$), $m = 1.80$, $ER_w = 30.30 \text{ } \Omega \cdot \text{m}$, $\tau = 1.50$, $n = 0.40$, and $p = 0.60$.

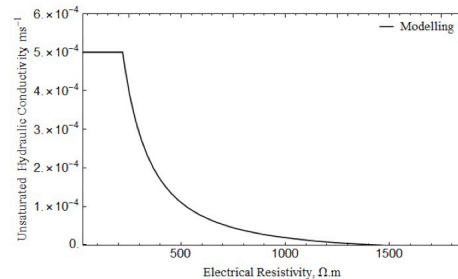


Figure 2. $k_{us}(ER)$ function for a sandy soil with parameters: $k_{sat} = 5.00 \times 10^{-4} \text{ m}^2 \cdot \text{s}^{-1}$, $\theta_r = 0.02 \text{ m}^3 \cdot \text{m}^{-3}$, $\theta_s = 0.45 \text{ m}^3 \cdot \text{m}^{-3}$, $m = 1.80$, $ER_w = 30.30 \text{ } \Omega \cdot \text{m}$, $\tau = 1.50$, $n = 0.40$, and $p = 0.60$.

To investigate the impact of the parameters on the hydrogeophysical model, six scenarios (Table 1) were constructed using the parameters from Figure 1 and Figure 2. The sensitivity of the models to changes in the hydraulic and petrophysical parameters (θ_r , θ_s , δ , m , p , and τ) was then analyzed.

4. Model validation for granular soils – sandy

The model's validation was performed using two granular soils with distinct electrical conductivity values. The first dataset consists of medium sand from this study, while the second dataset was obtained from Tuli & Hopmans (2003) and refers to fine sand.

The steps taken to validate the model involved: (1) collecting laboratory data on volumetric water content and electrical resistivity with identification of the saturated,

intermediate, and dry regions. (2) Determining the petrophysical parameters (m , p , and τ) through non-linear fitting of the $ER(\theta)$ function. (3) Determining the hydraulic parameter (δ) through minimization of the objective function. (4) Application – Determining the soil-water retention curve (SWRC) and unsaturated hydraulic conductivity function (k_{us}).

4.1 Case Study 1 - Soil with high electrical resistivity

The proposed hydrogeophysical model was verified using a granular material obtained from a civil construction project. The geotechnical classification and geoelectric (electrical resistivity) analysis values of the material were used in the model validation (Table 2). The classification was conducted following the guidelines of the American Society for Testing and Materials (ASTM) and the Brazilian Association of Technical Standards (ABNT).

Table 1. Result of the sensitivity analysis of the hydraulic and petrophysical parameters for the ERCC and $k_{us}(ER)$ functions.

Index	Modeled Scenarios	Analyzed Parameter	ERCC (Equation 9)	$k_{us}(ER)$ (Equation 10)
1	Increased soil residual volumetric water content	θ_r	Decrease in ER values for matric suctions greater than 10 kPa	Decrease in k_{us} for ER less than 1400 $\Omega.m$
2	Increased soil saturated volumetric water content	θ_s	Decrease in ER values for matric suctions below 1 kPa	Decrease in k_{us} for ER less than 500 $\Omega.m$
3	Increase in the wetting capacity of the soil and the matric suction value corresponding to the air-entry	δ	Decrease in air-entry point, and increase of the value of ER in this points	-
4	Increased interconnectivity between soil particles	m	Increase in ER values for all analyzed matric suction interval	Increase in k_{us} for ER great than 500 $\Omega.m$
5	Increased degree of saturation	p	Increase in the ER values for matric suctions above the air-entry point and changes in air-entry values	Increase in k_{us} values for all modeled resistivity range
6	Increased soil tortuosity	τ	Increase in the ER values for all analyzed matric suction range	Increase of more than one order of magnitude of k_{us} values for ER less than 1000 $\Omega.m$

Table 2. Geotechnical and geoelectric characterization of the Soil 1.

Informations/Data		Value
Case Study		Soil 1
Origin of soil		Brazil - Civil construction
Number of samples analyzed		6
Soil texture	Sand	1.00
	Silt	-
	Clay	-
Specific mass, ($kg.m^{-3}$)		1550
Porosity- n , (adm)		0.44
Saturated permeability- k_{sat} , ($m.s^{-1}$)		2.40×10^{-4}
Fluid electrical conductivity- EC_w , ($S.m^{-1}$)		4.28×10^{-3}
Fluid electrical resistivity- ER_w , ($\Omega.m$)		232.56
Volumetric Water Content, ($m^3.m^{-3}$)	θ_r	0.01
	θ_s	0.44

The relationship between the volumetric water content and matric suction (Table 3) was determined through a pressure plate test conducted in a Richards chamber that was equipped with a Pressure Plate Extractor 1500 F2 (Soilmoisture Equipment Corp®), following the procedures outlined in Dane & Topp (2002). The test assumed that the sample volume remained constant throughout.

A temperature-controlled room at 21 °C was used to assemble a geoelectric box for measuring the electrical potential (in volts). The granular material was packed into an acrylic box with dimensions of 0.20 m × 0.08 m × 0.80 m and a thickness of 0.40×10^{-2} m. The box was then connected in series to an adjustable direct current (DC) source (0 V-30 V/0 A-3 A/PS-4000, Icel®) with two multimeters. One multimeter was used to measure the potential difference, while the other measured the electric current being injected into the system. Silver electrodes with a sodium chloride coating, 0.25×10^{-1} m long and spaced at 0.64×10^{-1} m, were used to prevent electrode polarization problems under low-frequency conditions, following the recommendation of Telford et al. (1990).

The potential difference was measured using the Wenner acquisition geometry with a geometric factor of 0.41 m. For each electrical potential measurement, three soil samples were collected, and the gravimetric water content was determined following the guidelines of ASTM (2010) and ABNT (2016). Then, the electrical resistivity values were calculated for each volumetric water content value (Figure 3).

Table 3. Experimentally determined average values of the volumetric water content and matric suction determined in a pressure chamber (Soil 1).

ψ (kPa)	θ ($\text{m}^3 \cdot \text{m}^{-3}$)
P _{atm}	0.44
2	0.08
4	0.06
6	0.05
8	0.05
10	0.05
14	0.04
20	0.04
30	0.03
40	0.04
60	0.03
80	0.03
100	0.03
150	0.03
200	0.02
300	0.03
350	0.02
600	0.02
1000	0.01
1500	0.02

The experimentally determined average values of the volumetric water content indicated three distinct regions as the electrical resistivity increased: the saturated, intermediate, and dry regions, which corresponded to electrical resistivities of $665.53 \Omega \cdot \text{m} \leq ER \leq 734.64 \Omega \cdot \text{m}$, $920.88 \Omega \cdot \text{m} \leq ER \leq 1909.11 \Omega \cdot \text{m}$, and $1909.11 \Omega \cdot \text{m} \leq ER < 2296.13 \Omega \cdot \text{m}$, respectively (Figure 3).

The experimental data obtained in the laboratory (Figure 3) were fitted to the non-linear model (Equation 8) to obtain the petrophysical parameters m , p , and τ , which are responsible for the interconnectivity between soil particles, the degree of saturation, and tortuosity of the soil, respectively.

In the region where the volumetric water content equals the saturated water content (θ_s) and the electrical resistivity is lower than $ER_w \cdot \theta_s^{-p} \cdot \tau \cdot m^{-M+p}$, which corresponds to $553.88 \Omega \cdot \text{m}$ – the saturated region, the expected physical behavior of low electrical resistivities associated with the volumetric water content is observed. However, for $553.88 \Omega \cdot \text{m} \leq ER \leq 1300 \Omega \cdot \text{m}$, an abrupt decrease in the volumetric water content is noted, and it approaches the residual when $ER \geq 2300 \Omega \cdot \text{m}$ (Figure 4).

The $k_{us}(ER)$ function displays the maximum values of unsaturated hydraulic conductivity (approximately $2.40 \times 10^{-4} \text{ ms}^{-1}$) linked with the electrical resistivity when ER is less than or equal to $553.88 \Omega \cdot \text{m}$, which represents

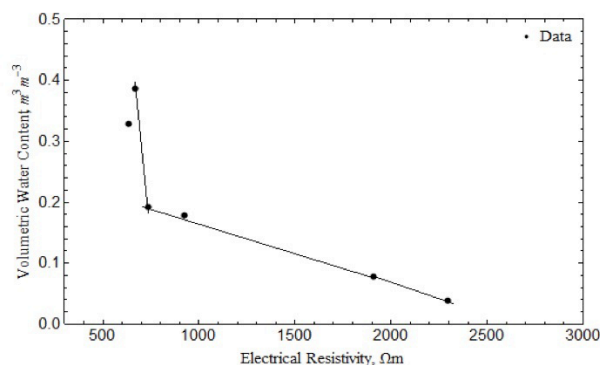


Figure 3. Theoretical piecewise linear relationship between volumetric water content and electrical resistivity for Soil 1

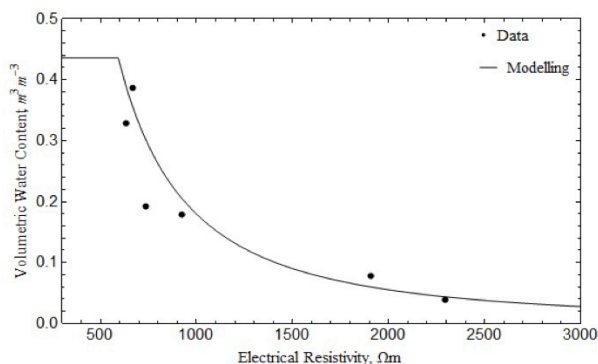


Figure 4. Adjustment of the $\theta(ER)$ function applied to soil data resulting in $m = 1.00$, $p = 0.59$, and $\tau = 1.11$ (Soil 1).

the soil at the saturation region (Figure 5). In the case of $553.88 \Omega \cdot m \leq ER \leq 2000 \Omega \cdot m$, there is a significant variation in the unsaturated hydraulic conductivity associated with the unsaturated soil. When ER is greater than or equal to $2000 \Omega \cdot m$, the unsaturated hydraulic conductivity remains almost constant, which indicates dry soil.

To determine the hydraulic parameter (δ) that affects the wetting ability of the soil, an inverse problem formulation was employed. In this case, the aim was to minimize a function to find the value of δ that best represents the medium, and subsequently, determine the SWRC and the unsaturated hydraulic conductivity function.

The inverse problem was solved by using an objective function that quantifies the difference between the laboratory measurements and the values calculated using Equation 9. The objective function is defined as follows:

$$OF(ER) = (ER_M - ER_C)^2 \quad (11)$$

where ER_M = the experimentally measured electrical resistivity; and ER_C = the computed values for each value of parameter δ . The goal is to estimate the values of the parameters that best represent the soil condition by minimizing this function. It is assumed that all parameters in Equation 9, except δ , are constant based on the available information.

An algorithm was implemented to solve this objective function, where $ER(\psi)$ is computed for each value of δ . These computed values are subtracted from the corresponding experimentally measured values and the difference is squared. The estimated value with the smallest squared residual is then chosen (Equation 11).

A range of less than 10 kPa was examined to minimize the objective function. The selected points (Table 4) represent a range of intermediate electrical resistivity with low matric suction and a range of high resistivity with varying matric suction.

The $ER(\psi)$ function for each point exhibits a region of minimal points that correspond to different values of δ . A point where the quadratic residue is minimum is identified (Figure 6), and it is observed that Point 1 has the smallest quadratic residue. Therefore, the optimal parameter value of δ that best represents this sandy soil with the given geotechnical characteristics is 0.46 kPa^{-1} .

With the value of δ , it is possible to construct the soil water retention curve (SWRC) (Figure 7a) and unsaturated hydraulic conductivity curve (Figure 7b) of soil 1 with the identification of the air-entry point ($\psi_{air} = 0.39 \text{ kPa}$) calculated by Equation 4. The data obtained from the pressure plate tests are displayed in Table 3.

The SWRC (Figure 7a) exhibits agreement with the experimental data, indicating the feasibility of obtaining SWRC through indirect measurements of the studied Soil 1.

The accuracy of the proposed hydrogeophysical model in predicting the soil water retention curve and unsaturated hydraulic conductivity curve of soil through electrical resistivity measurements is demonstrated by the good agreement between the model predictions and the experimental values of volumetric water content and electrical potential obtained using pressure plate tests and a geoelectrical box.

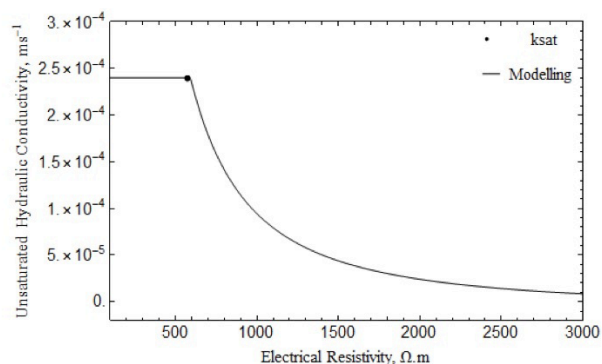


Figure 5. $k_{us}(ER)$ function curve for Soil 1 with parameters $m = 1$, $p = 0.59$, and $\tau = 1.11$.

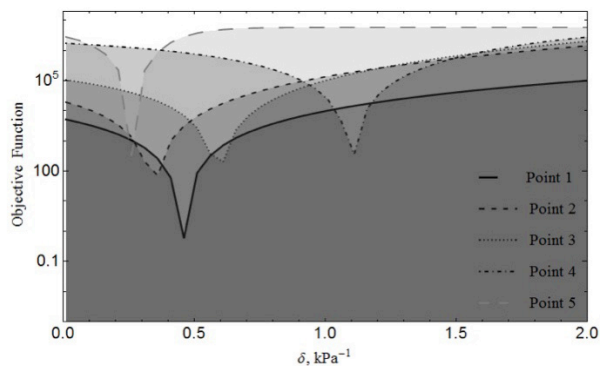


Figure 6. Minimization of the $ER(\psi)$ function for Points 1 to 5 – soil 1.

Table 4. Points used in the minimization process and the corresponding values of δ_{min} for Soil 1.

Point	ψ (kPa)	ER_M ($\Omega \cdot m$)	δ_{min} (kPa^{-1})
1	0.45	665.53	0.46
2	1.11	734.64	0.36
3	1.33	920.88	0.61
4	2.00	1909.11	1.11
5	10.00	2296.13	0.26

Table 5. Geotechnical and geoelectric characterization of the Soil 2 (modified from Tuli & Hopmans, 2003).

Informations/Data		Value
Case Study		Soil 2
Origin of soil		USA - Osa Flaco
Number of samples analyzed		20
Soil texture	Sand	1.00
	Silt	-
	Clay	-
Specific mass, (kg.m ⁻³)		1550
Porosity- <i>n</i> , (adm)		0.41
Saturated permeability- <i>k_{sat}</i> , (m.s ⁻¹)		1.13 × 10 ⁻⁵
Fluid electrical conductivity- <i>EC_w</i> , (S.m ⁻¹)		2.50 × 10 ⁻¹
Fluid electrical resistivity- <i>ER_w</i> , (Ω.m)		4
Volumetric Water Content, (m ³ .m ⁻³)	θ _r	0.07
	θ _s	0.41

Table 6. Experimentally obtained average values of the volumetric water content and matric suction using the multistep outflow method for Soil 2 (modified from Tuli & Hopmans, 2003).

ψ (kPa)	θ (m ³ .m ⁻³)
0.01	0.41
0.72	0.38
0.63	0.37
0.74	0.34
0.81	0.34
0.83	0.31
1.04	0.30
1.04	0.28
0.93	0.28
1.17	0.23
1.17	0.21
1.46	0.16
1.46	0.15
1.89	0.11
2.00	0.10
6.34	0.08

4.2 Case Study 2 – Soil with low electrical resistivity

Tuli & Hopmans (2003) investigated the correlation between various transport coefficients and pore geometrical properties, and measured the hydraulic and electrical conductivity of Oso Flaco sand (Table 5) at different levels of saturation for four fluid conductivities. For this study, the data of the saturated samples using a CaCl₂ solution (electrical conductivity 2.5×10⁻¹ S.m⁻¹) were utilized.

The soil samples were packed uniformly into brass columns (6.00×10⁻² m high and 8.25 × 10⁻² m inner diameter) with a wet strength fast flow filter paper glued at the bottom. The filter paper was soaked in CaCl₂ solution, which was maintained about 0.01 m below the rims of the columns. The filter paper was then removed, and the saturated soil

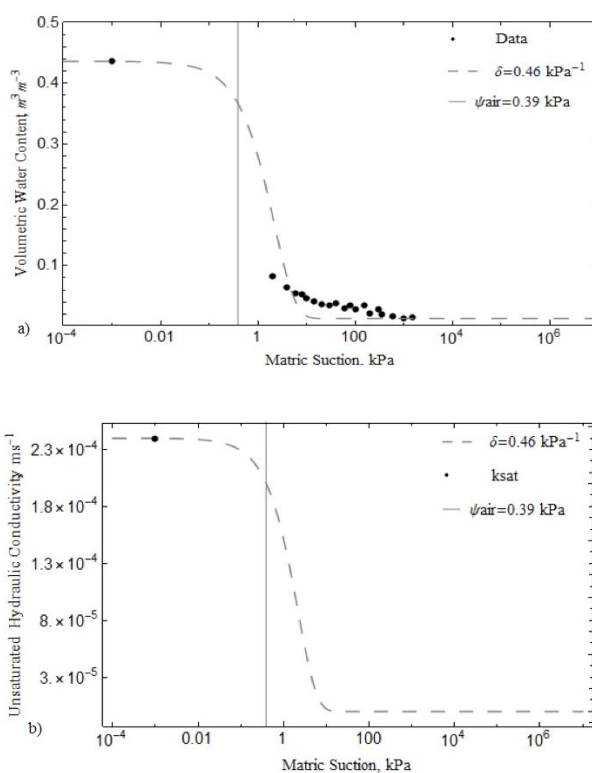


Figure 7. (a) SWRC and (b) unsaturated hydraulic conductivity function for the value of δ obtained by minimization (Soil 1).

samples were assembled in Tempe Pressure Cells to estimate the soil-water retention curve (Table 6) and unsaturated hydraulic conductivity function using the multistep outflow method, as described by Tuli & Hopmans (2003).

A miniature tensiometer and a two-rod TDR mini probe were vertically inserted into the center of each soil sample after assembly of the Tempe pressure cells. The samples were then resaturated with the solution through the bottom porous membrane assembly and allowed to equilibrate with

the applied pressure. Electrical conductivity values were determined using the Time Domain Reflectometry (TDR) method, as described by Tuli & Hopmans (2003).

TDR is a technique that uses the propagation of electromagnetic waves to indirectly measure moisture content by correlating it with the electric and dielectric properties of geomaterials. The travel time is associated with the charge storage capacity of the soil and the volumetric water content. TDR measurements involve transmitting an impulse and observing the response within a certain time interval.

The Time Domain Reflectometer (TDR) measures the round-trip time of an electromagnetic wave that is reflected by the medium being tested. It then converts this time into a distance unit and displays the information as a waveform. The time interval between these reflections can be used to calculate the velocity of the electromagnetic wave in the medium. Additionally, TDR waveform measurements can be transformed into electrical conductivity using algorithms. Tuli & Hopmans (2003) utilized a Tektronix 1502B metallic cable-tester and WinTDR99 software to analyze the waveforms.

Using the data from Tuli & Hopmans (2003), it was feasible to distinguish four distinct regions based on electrical resistivity ranges: saturated, intermediate 1, intermediate 2 and dry. These regions correspond to resistivity ranges of $11.11 \Omega \cdot m \leq ER \leq 39.23 \Omega \cdot m$, $39.23 \Omega \cdot m < ER \leq 86.73$, $86.73 \Omega \cdot m < ER \leq 95.96 \Omega \cdot m$, and $95.96 \Omega \cdot m < ER < 125.28 \Omega \cdot m$, respectively (Figure 8).

By employing the same methodology presented in Case Study 1, it was feasible to determine the petrophysical parameters m , p , and τ , and consequently, simulate the performance of the $\theta(ER)$ and $k_{is}(ER)$ functions.

In Figure 9, the saturated region, where $\theta(ER) = 44.33\%$, corresponds to electrical resistivity values ranging from $11.11 \Omega \cdot m$ to $31.32 \Omega \cdot m$. An abrupt decline in the volumetric water content occurs when the electrical resistivity ranges from $31.32 \Omega \cdot m$ to $100 \Omega \cdot m$. Conversely, for electrical resistivity values greater than $150 \Omega \cdot m$, the volumetric water content approaches the residual level.

Figure 10 displays the maximum values of unsaturated hydraulic conductivity (approximately $1.13 \times 10^{-5} m \cdot s^{-1}$), which are linked to electrical resistivity values of $ER \leq 31.32 \Omega \cdot m$, corresponding to the saturation region of the soil. In the unsaturated soil region, significant variability in the unsaturated hydraulic conductivity is evident for $31.32 \Omega \cdot m \leq ER \leq 100 \Omega \cdot m$. As for ER values greater than or equal to $100 \Omega \cdot m$, the unsaturated hydraulic conductivity drops to its minimum level, indicating dry soil conditions.

By applying the same methodology employed in Case Study 1, the hydraulic parameter δ was ascertained by minimizing the objective function (Equation 11). Various scenarios of electrical resistivity and pressure were considered for the data points chosen within the range of less than 10 kPa (see Table 7).

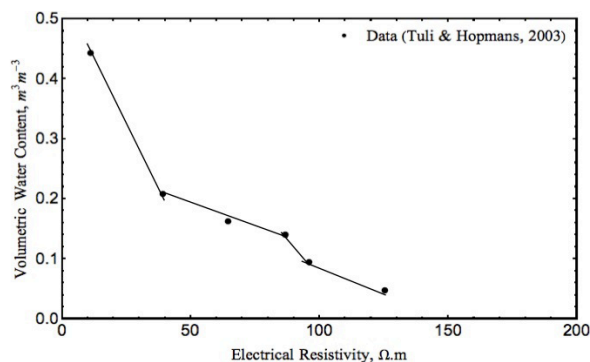


Figure 8. Theoretical piecewise linear relationship between volumetric water content and electrical resistivity for Soil 2.

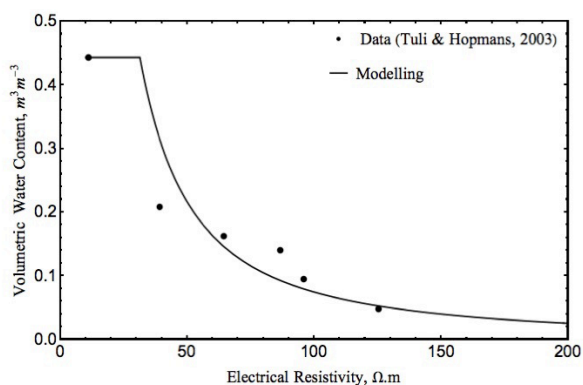


Figure 9. Adjustment of the $\theta(ER)$ function applied to soil data resulting in $m = 1.79$, $p = 0.65$, and $\tau = 1.67$ (Soil 2).

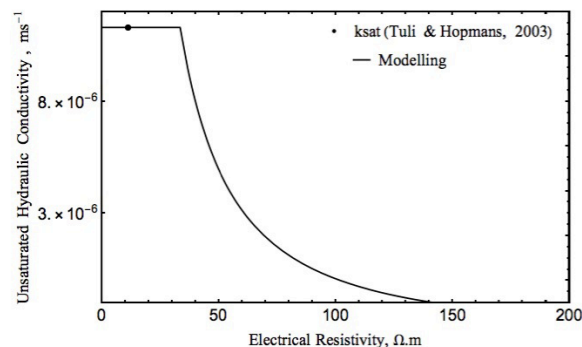


Figure 10. $k_{is}(ER)$ function curve for Soil 2 with parameters $m=1.79$, $p=0.65$, and $\tau=1.67$.

Figure 11 shows a cluster of points where the quadratic residue varies according to different values of δ , with one point exhibiting the lowest quadratic residue. These findings suggest that Point 4 yields the minimum quadratic residue, implying that the most suitable δ parameter for this sandy soil with its respective geotechnical features is $0.56 kPa^{-1}$.

Table 7. Points used in the minimization process and the corresponding values of δ_{min} – Soil 2 (modified from Tuli & Hopmans, 2003).

Point	ψ (kPa)	ER_M ($\Omega \cdot m$)	δ_{min} (kPa^{-1})
1	0.001	11.11	*
2	1	39.22	0.31
3	2	64.43	0.76
4	5	86.73	0.56
5	6.5	95.96	0.61

* not found.

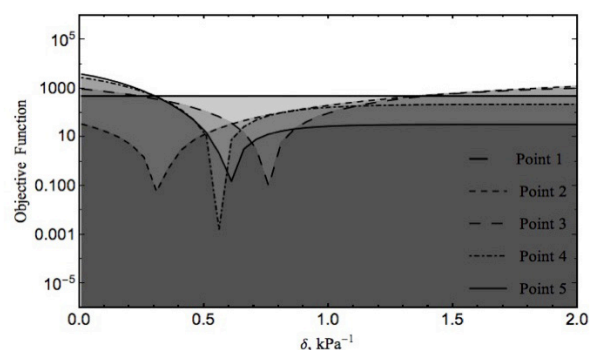


Figure 11. Minimization of the $ER(\psi)$ function for Points 1 to 5 (Soil 2).

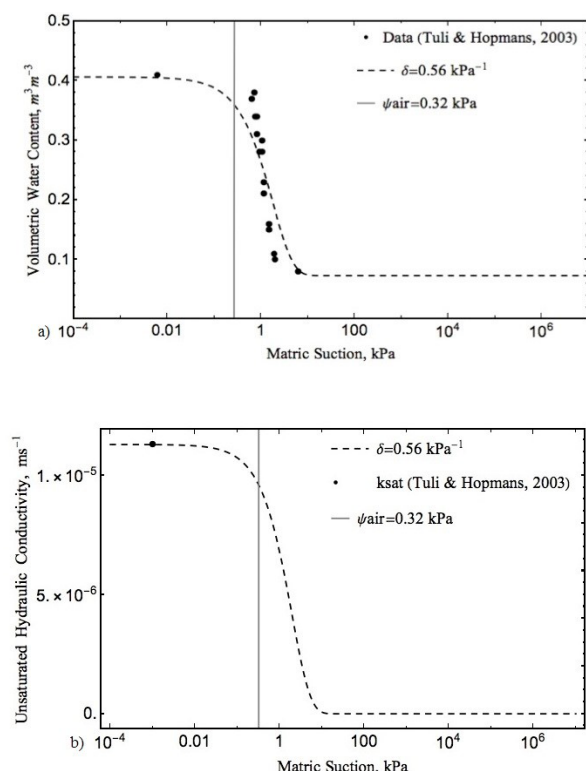


Figure 12. (a) SWRC and (b) unsaturated hydraulic conductivity function for the value of δ obtained by minimization Soil 2.

By using the δ value obtained, it is feasible to generate the SWRC (Figure 12a) and the unsaturated hydraulic conductivity curve (Figure 12b) for Soil 2. Additionally, the air-entry point ($\psi_{air} = 0.32$ kPa), determined using Equation 4, can be identified.

The outcomes illustrated in Figures 12a and 12b for Soil 2 demonstrate a consistent agreement with the findings obtained for Soil 1. Therefore, it is feasible to represent the SWRC and unsaturated hydraulic conductivity function using indirect measurements. The hydrogeophysical model proposed in this study was validated by TDR measurements for soil with low electrical resistivity.

5. Conclusion

A semi-analytical unsaturated hydrogeophysical constitutive model was formulated, which integrates aspects of geotechnics, hydrogeology, petrophysics, and geophysics. The purpose of this model is to enhance hydrogeological characterization and soil matrix monitoring. The model enables indirect estimation of soil water retention and unsaturated hydraulic conductivity curves by using direct current electrical resistivity measurements (as applied in this study) and TDR measurements (based on literature data from Tuli & Hopmans (2003)). The model is founded on the integration of hydromechanical and petrophysical models, thereby providing a means of describing soil hydrogeophysical characteristics that are crucial to civil engineering projects.

The estimation of the $ERCC$ and unsaturated hydraulic conductivity as a function of electrical resistivity has significant practical applications. The effectiveness of the proposed model was verified through examination of a granular material characterized from geotechnical, geophysical, and hydrodynamic perspectives. Using direct measurements and minimizing the objective function, the hydraulic and petrophysical parameters governing the soil-water retention and unsaturated hydraulic conductivity curves as a function of matric suction were ascertained. Remarkably, the model outputs exhibited good agreement with experimental data.

The laboratory experiments conducted in Case Studies 1 and 2 utilized low-cost instrumentation and TDR, respectively, and yielded satisfactory outcomes, thus proving the practical feasibility of these methods for monitoring the state of soils over extensive spatial and temporal scales. Moreover, indirect measurement of soil properties can facilitate high-density spatial sampling of soils and the ability to rapidly and indirectly determine soil conditions, while being more cost-effective compared to direct measurement methods.

The petrophysical parameters determined for the soils provide insight into their physical conditions. For Case Study 1 (medium sand), the hydraulic parameter value is lower compared to that in Case Study 2, resulting in different air-entry values. In contrast, for Case Study 2 (fine sand), the parameters governing the degree of cementation and tortuosity are higher than those in Case Study 1.

The findings of this study may prove valuable to researchers involved in geoscience/geophysics, civil engineering/geotechnology, and agronomy, as they can benefit greatly from the ability to rapidly and indirectly determine soil conditions based on either the SWRC or unsaturated hydraulic conductivity function.

Readers intending to utilize this model should take note that the theoretical framework was based on simplifications regarding water distribution in the soil, the absence of clay in the soil, and fixed values of void ratio, porosity, and specific mass. Therefore, the model may need to be adjusted for soils containing clay or demonstrating significant surface conduction. Also, to broaden the scope of the model, additional laboratory tests are recommended to validate its applicability.

Acknowledgements

This study was financed in part by the Coordination for the Improvement of Higher Education Personnel (CAPES - Finance Code 001). The authors also acknowledge the support of the National Council for Scientific and Technological Development (CNPq - Grant 305484/2020-6), the Foundation for Research Support of the Federal District (FAPDF - Grant 00193.00000920/2021-12), the National Electric Energy Agency (ANEEL) and its R&D partners Neoenergia/CEB Distribuição S.A. (AINOA: A System to Monitor Internal Pathologies in Earth and Rockfill Dams Based on Artificial Intelligence and Internet-of-Things: A Case study of the Paranoá Dam-Grant number PD-05160- 1904/2019, contract CEBD782/2019), the EMBRAPA Instrumentação (Acordo de Cooperação, DOU n° 240, 22 de dezembro de 2022) and the University of Brasília, including the Laboratory of the Physics and Chemistry of Soils of the School of Agronomy, the Laboratory of Applied Geophysics, and the Laboratory of Geochemistry of the Institute of Geosciences.

Declaration of interest

The authors have no conflict of interest regarding the matter included in this paper. All co-authors have observed and affirmed the contents of the paper and there is no financial interest to report.

Authors' contributions

Manuelle Santos Góis: conceptualization, methodology, formal analysis, writing – original draft, Writing – review & editing, Investigation. Katherin Rocio Cano Bezerra da Costa: methodology, formal analysis, writing – original draft, writing – review & editing, Investigation. André Luís Brasil Cavalcante: conceptualization, formal analysis, writing – original draft, writing – review & editing, Investigation.

Data availability

All data produced or examined in the course of the current study are included in this article.

List of symbols

g	Gravitational acceleration
k_{sat}	Saturated hydraulic conductivity of the soil
$k_z(\theta)$	Function of the unsaturated hydraulic conductivity in terms of the volumetric water content in the z-direction
m	Cementation exponent
n	Porosity
p	Saturation exponent
t	Time
z	Direction
DC	Direct current
EC	Electrical conductivity
EC_w	Fluid electrical conductivity
ER	Electrical resistivity
ERC	Computed values electrical resistivity
$ERCC$	Electrical Resistivity Characteristic Curve
ERM	Experimentally measured electrical resistivity
ER_w	Fluid electrical resistivity
S_w	Fractional water saturation
$SWRC$	Soil Water Retention Curve
TDR	Time Domain Reflectometry
δ	Hydraulic adjustment parameter
θ	Volumetric soil water content
θ_r	Volumetric soil water content in the residual state
$\theta_s - \theta_r$	Maximum soil wetting capacity
θ_s	Volumetric soil water content in the saturated state
ρ_w	Water density
τ	Tortuosity
ψ	Soil suction
ψ_{air}	Air-entry soil suction
$\partial\psi/\partial\theta$	Variation in the matric suction in relation to the volumetric water content

References

- ABNT NBR 6457. (2016). *Amostras de Solo — Preparação para Ensaios de Compactação e Ensaios de Caracterização*. ABNT - Associação Brasileira de Normas Técnicas, Rio de Janeiro, RJ.
- Albuquerque, E.A.C., Borges, L.P.D.F., Cavalcante, A.L.B., & Machado, S.L. (2022). Prediction of soil water retention curve based on physical characterization parameters using machine learning. *Soils and Rocks*, 45(3), e2022000222. <http://dx.doi.org/10.28927/SR.2022.000222>.
- Archie, G.E. (1942). The electrical resistivity log as an aid in determining some reservoir characteristics. *Transactions of the AIME*, 146(1), 54-62. <https://doi.org/10.2118/942054-G>.
- ASTM D2216-19. (2010). *Standard Test Methods for Laboratory Determination of Water (Moisture) Content of Soil and Rock by Mass*. ASTM International, West Conshohocken, PA. <https://doi.org/10.1520/D2216-19>.
- Binley, A., Hubbard, S.S., Huisman, J.A., Revil, A., Robinson, D.A., Singha, K., & Slater, L.D. (2015). The emergence of hydrogeophysics for improved understanding of subsurface processes over multiple scales. *Water Resources Research*, 51(6), 3837-3866. <http://dx.doi.org/10.1002/2015WR017016>.
- Briaud, J.L. (2013). *Geotechnical engineering: unsaturated and saturated soils*. John Wiley & Sons. <https://doi.org/10.1002/9781118686195>.
- Brooks, R.H., & Corey, A.T. (1964). *Hydraulic properties of porous media* (Hydrology Papers, No. 3). Colorado State University.
- Butler, D.K. (2005). *Near-surface geophysics* (SEG investigations in geophysics series, No. 13). Society of Exploration Geophysicists. <https://doi.org/10.1190/1.9781560801719>.
- Camapum de Carvalho, J., & Gitirana Junior, G.D.F. (2021). Unsaturated soils in the context of tropical soils. *Soils and Rocks*, 44, 1-25. <http://dx.doi.org/10.28927/SR.2021.068121>.
- Carbajal, E.J., Diniz, M.D.S., Rodriguez-Pacheco, R.L., & Cavalcante, A.L.B. (2022). Contaminant transport model in transient and unsaturated conditions applied to laboratory column test with tailings. *Soils and Rocks*, 45, e2022076021. <http://dx.doi.org/10.28927/SR.2022.076021>.
- Cardoso, R., & Dias, A.S. (2017). Study of the electrical resistivity of compacted kaolin based on water potential. *Engineering Geology*, 226, 1-11. <http://dx.doi.org/10.1016/j.enggeo.2017.04.007>.
- Cavalcante, A.L.B., & Mascarenhas, P.V.S. (2021). Efficient approach in modeling the shear strength of unsaturated soil using soil water retention curve. *Acta Geotechnica*, 16, 3177-3186. <http://dx.doi.org/10.1007/s11440-021-01144-6>.
- Cavalcante, A.L.B., & Zornberg, J.G. (2017). Efficient approach to solving transient unsaturated flow problems. I: analytical solutions. *International Journal of Geomechanics*, 17(7), 04017013-1-04017013-17. [http://dx.doi.org/10.1061/\(ASCE\)GM.1943-5622.0000875](http://dx.doi.org/10.1061/(ASCE)GM.1943-5622.0000875).
- Cavalcante, A.L.B., Borges, L.P.D.F., & Zornberg, J.G. (2019). New 3D analytical solution for modeling transient unsaturated flow due to wetting and drying. *International Journal of Geomechanics*, 19(7), 04019077. [http://dx.doi.org/10.1061/\(ASCE\)GM.1943-5622.0001461](http://dx.doi.org/10.1061/(ASCE)GM.1943-5622.0001461).
- Cho, S.E. (2016). Stability analysis of unsaturated soil slopes considering water-air flow caused by rainfall infiltration. *Engineering Geology*, 211, 184-197. <http://dx.doi.org/10.1016/j.enggeo.2016.07.008>.
- Chou, Y., & Wang, L. (2021). Soil-water characteristic curve and permeability coefficient prediction model for unsaturated loess considering freeze-thaw and dry-wet. *Soils and Rocks*, 44(1), e2021058320. <http://dx.doi.org/10.28927/SR.2021.058320>.
- Costa, M.B.A.D., & Cavalcante, A.L.B. (2020). Novel approach to determine soil-water retention surface. *International Journal of Geomechanics*, 20(6), 04020054-1-04020054-9. [http://dx.doi.org/10.1061/\(ASCE\)GM.1943-5622.0001684](http://dx.doi.org/10.1061/(ASCE)GM.1943-5622.0001684).
- Crawford, M.M., Bryson, L.S., Woolery, E.W., & Wang, Z. (2019). Long-term landslide monitoring using soil-water relationships and electrical data to estimate suction stress. *Engineering Geology*, 251, 146-157. <http://dx.doi.org/10.1016/j.enggeo.2019.02.015>.
- Dane, J.H., & Topp, G.C. (2002). *Methods of soil analysis, Part 4 physical methods*. Soil Science Society of America, Inc. <https://doi.org/10.2136/sssabookser5.4>.
- Datsios, Z.G., Mikropoulos, P.N., & Karakousis, I. (2017). Laboratory characterization and modeling of DC electrical resistivity of sandy soil with variable water resistivity and content. *IEEE Transactions on Dielectrics and Electrical Insulation*, 24(5), 3063-3072. <http://dx.doi.org/10.1109/TDEI.2017.006583>.
- Di Maio, R., Piegari, E., Todero, G., & Fabbrocino, S. (2015). A combined use of Archie and van Genuchten models for predicting hydraulic conductivity of unsaturated pyroclastic soils. *Journal of Applied Geophysics*, 112, 249-255. <http://dx.doi.org/10.1016/j.jappgeo.2014.12.002>.
- Doussan, C., & Ruy, S. (2009). Prediction of unsaturated soil hydraulic conductivity with electrical conductivity. *Water Resources Research*, 45(10), W10408. <http://dx.doi.org/10.1029/2008WR007309>.
- Ewing, R.P., & Hunt, A.G. (2006). Dependence of the electrical conductivity on saturation in real porous media. *Vadose Zone Journal*, 5(2), 731-741. <http://dx.doi.org/10.2136/vzj2005.0107>.
- Fredlund, D.G. (2021). Myths and misconceptions related to unsaturated soil mechanics. *Soils and Rocks*, 44(3), e2021062521. <http://dx.doi.org/10.28927/SR.2021.062521>.
- Fredlund, D.G., & Rahardjo, H. (1993). *Soil mechanics for unsaturated soils*. John Wiley & Sons. <https://doi.org/10.1002/9780470172759>.
- Fredlund, D.G., & Xing, A. (1994). Equations for the soil-water characteristic curve. *Canadian Geotechnical Journal*, 31(4), 521-532. <http://dx.doi.org/10.1139/t94-061>.

- Friedman, S.P. (2005). Soil properties influencing apparent electrical conductivity: a review. *Computers and Electronics in Agriculture*, 46(1-3), 45-70. <http://dx.doi.org/10.1016/j.compag.2004.11.001>.
- Fu, Y., Horton, R., & Heitman, J.L. (2021a). Estimation of soil water retention curves from soil bulk electrical conductivity and water content measurements. *Soil & Tillage Research*, 209, <http://dx.doi.org/10.1016/j.still.2021.104948>.
- Fu, Y., Horton, R., Ren, T., & Heitman, J.L. (2021b). A general form of Archie's model for estimating bulk soil electrical conductivity. *Journal of Hydrology (Amsterdam)*, 597, <http://dx.doi.org/10.1016/j.jhydrol.2021.126160>.
- Glover, P.W.J. (2010). A generalized Archie's law for n phases. *Geophysics*, 75(6), E247-E265.
- Glover, P.W.J. (2015). 11.04—geophysical properties of the near surface earth: electrical properties. In G. Schubert (Ed.), *Treatise on geophysics* (Vol. 11, pp. 89-137). <https://doi.org/10.1016/B978-0-444-53802-4.00189-5>.
- Glover, P.W.J., Hole, M.J., & Pous, J. (2000). A modified Archie's law for two conducting phases. *Earth and Planetary Science Letters*, 180(3-4), 369-383. [http://dx.doi.org/10.1016/S0012-821X\(00\)00168-0](http://dx.doi.org/10.1016/S0012-821X(00)00168-0).
- Hinnell, A.C., Ferré, T.P.A., Vrugt, J.A., Huisman, J.A., Moysey, S., Rings, J., & Kowalsky, M.B. (2010). Improved extraction of hydrologic information from geophysical data through coupled hydrogeophysical inversion. *Water Resources Research*, 46(4), <http://dx.doi.org/10.1029/2008WR007060>.
- Hong-jing, J., Shun-qun, L., & Lin, L. (2014). The relationship between the electrical resistivity and saturation of unsaturated soil. *The Electronic Journal of Geotechnical Engineering*, 19, 3739-3746.
- Hubbard, S.S., & Rubin, Y. (2005). Introduction to hydrogeophysics. In Y. Rubin & S.S. Hubbard (Eds.), *Hydrogeophysics. Water Science and Technology Library* (pp. 3-21). Springer. https://doi.org/10.1007/1-4020-3102-5_1.
- Keller, G.V. (1988). 2. Rock and mineral properties. In M.N. Nabighian (Ed.), *Electromagnetic methods in applied geophysics* (pp. 13-52). Society of Exploration Geophysicists. <https://doi.org/10.1190/1.9781560802631.ch2>.
- Keller, G.V., & Frischknecht, F.C. (1966). *Electrical methods in geophysical prospecting*. Pergamon Press.
- Kibria, G., & Hossain, M.S. (2012). Investigation of geotechnical parameters affecting electrical resistivity of compacted clays. *Journal of Geotechnical and Geoenvironmental Engineering*, 138(12), 1520-1529. [http://dx.doi.org/10.1061/\(ASCE\)GT.1943-5606.0000722](http://dx.doi.org/10.1061/(ASCE)GT.1943-5606.0000722).
- Kong, L.W., Sayem, H.M., Zhang, X.W., & Yin, S. (2017). Relationship between electrical resistivity and matric suction of compacted granite residual soil. In *Proceedings of the PanAm unsaturated soils 2017: swell-shrink and tropical soils* (pp. 430-439). ASCE. <https://doi.org/10.1061/9780784481707.043>.
- Lai, W., & Ogden, F.L. (2015). A mass-conservative finite volume predictor-corrector solution of the 1D Richards' equation. *Journal of Hydrology (Amsterdam)*, 523, 119-127. <http://dx.doi.org/10.1016/j.jhydrol.2015.01.053>.
- Lesmes, D.P., & Friedman, S.P. (2005). Relationships between the electrical and hydrogeological properties of rocks and soils. In Y. Rubin & S. S. Hubbard (Eds.), *Hydrogeophysics* (pp. 87-128). Water Science and Technology Library. https://doi.org/10.1007/1-4020-3102-5_4.
- Libardi, P.L. (2005). *Dinâmica da água no solo* (Vol. 61). Edusp.
- Lima, O.A.L. (2014). *Propriedades físicas das rochas-bases da geofísica aplicada*. Sociedade Brasileira de Geofísica.
- Liu, H.H. (2017). Theory and applications of transport in porous media. In S. Majid Hassanizadeh & J. Bear (Eds.), *Fluid flow in the subsurface. History, generalization and applications of physical laws* (Vol. 28). Springer.
- Lu, D., Wang, H., Huang, D., Li, D., & Sun, Y. (2020). Measurement and estimation of water retention curves using electrical resistivity data in porous media. *Journal of Hydrologic Engineering*, 25(6), [http://dx.doi.org/10.1061/\(ASCE\)HE.1943-5584.0001925](http://dx.doi.org/10.1061/(ASCE)HE.1943-5584.0001925).
- Mawer, C., Knight, R., & Kitanidis, P.K. (2015). Relating relative hydraulic and electrical conductivity in the unsaturated zone. *Water Resources Research*, 51(1), 599-618. <http://dx.doi.org/10.1002/2014WR015658>.
- Mualem, Y., & Friedman, S.P. (1991). Theoretical prediction of electrical conductivity in saturated and unsaturated soil. *Water Resources Research*, 27(10), 2771-2777. <http://dx.doi.org/10.1029/91WR01095>.
- Niu, Q., Fratta, D., & Wang, Y.H. (2015). The use of electrical conductivity measurements in the prediction of hydraulic conductivity of unsaturated soils. *Journal of Hydrology (Amsterdam)*, 522, 475-487. <http://dx.doi.org/10.1016/j.jhydrol.2014.12.055>.
- Piegari, E., & Di Maio, R. (2013). Estimating soil suction from electrical resistivity. *Natural Hazards and Earth System Sciences*, 13(9), 2369-2379. <http://dx.doi.org/10.5194/nhess-13-2369-2013>.
- Revil, A., Karaoulis, M., Johnson, T., & Kemna, A. (2012). Review: some low-frequency electrical methods for subsurface characterization and monitoring in hydrogeology. *Hydrogeology Journal*, 20(4), 617-658. <http://dx.doi.org/10.1007/s10040-011-0819-x>.
- Rhoades, J.D., Raats, P.A.C., & Prather, R.J. (1976). Effects of liquid-phase electrical conductivity, water content, and surface conductivity on bulk soil electrical conductivity. *Soil Science Society of America Journal*, 40(5), 651-655. <http://dx.doi.org/10.2136/sssaj1976.036159950040000500017x>.
- Richards, L.A. (1931). Capillary conduction of liquids through porous mediums. *Physics*, 1(5), 318-333. <http://dx.doi.org/10.1063/1.1745010>.
- Rinaldi, V.A., & Cuestas, G.A. (2002). Ohmic conductivity of a compacted silty clay. *Journal of Geotechnical and Geoenvironmental Engineering*, 128(10), 824-835. [http://dx.doi.org/10.1061/\(ASCE\)1090-0241\(2002\)128:10\(824\)](http://dx.doi.org/10.1061/(ASCE)1090-0241(2002)128:10(824)).

- Santamarina, J.C., Klein, A., & Fam, M.A. (2001). Soils and waves: particulate materials behavior, characterization and process monitoring. *Journal of Soils and Sediments*, 1(2), 130. <http://dx.doi.org/10.1007/BF02987719>.
- Shah, P.H., & Singh, D.N. (2005). Generalized Archie's law for estimation of soil electrical conductivity. *Journal of ASTM International*, 2(5), 1-20. <http://dx.doi.org/10.1520/JAI13087>.
- Sheng, D., Gens, A., Fredlund, D.G., & Sloan, S.W. (2008). Unsaturated soils: from constitutive modelling to numerical algorithms. *Computers and Geotechnics*, 35(6), 810-824. <http://dx.doi.org/10.1016/j.compgeo.2008.08.011>.
- Singha, K., Day-Lewis, F.D., Johnson, T., & Slater, L.D. (2014). Advances in interpretation of subsurface processes with time-lapse electrical imaging. *Hydrological Processes*, 29(6), 1549-1576. <http://dx.doi.org/10.1002/hyp.10280>.
- Telford, W.M., Geldart, L.P., & Sheriff, R.E. (1990). *Applied geophysics*. Cambridge University Press. <https://doi.org/10.1017/CBO9781139167932>.
- Tuli, A., & Hopmans, J.W. (2003). Effect of degree of fluid saturation on transport coefficients in disturbed soils. *European Journal of Soil Science*, 55(1), 147-164. <http://dx.doi.org/10.1046/j.1365-2389.2002.00493.x-i1>.
- van Genuchten, M.T. (1980). A closed-form equation for predicting the hydraulic conductivity of unsaturated soils. *Soil Science Society of America Journal*, 44(5), 892-898. <http://dx.doi.org/10.2136/sssaj1980.03615995004400050002x>.
- Zhang, Z., Wang, W., Yeh, T.C.J., Chen, L., Wang, Z., Duan, L., An, K., & Gong, C. (2016). Finite analytic method based on mixed-form Richards' equation for simulating water flow in vadose zone. *Journal of Hydrology (Amsterdam)*, 537, 146-156. <http://dx.doi.org/10.1016/j.jhydrol.2016.03.035>.